

Giant magneto-electric coupling in 100 nm thick Co capped by ZnO nanorods

G. Vinai,^a B. Ressel,^b P. Torelli,^a F. Loi,^c B. Gobaut,^d R. Ciancio,^a B. Casarin,^c A. Caretta,^d
L. Capasso,^d F. Parmigiani,^c F. Cugini,^e M. Solzi,^e M. Malvestuto^d and R. Ciprian^{d,*}

^aCNR-Istituto Officina dei Materiali IOM, s.s. 14 km 163.5, 34149, Trieste, Italy

^bUniversity of Nova Gorica, Vipavska Cesta 11c, Ajdovščina, 5270, Slovenia

^cUniversità degli Studi di Trieste, Via A. Valerio 2, 34127, Trieste, Italy.

^dElettra Sincrotrone di Trieste, s.s. 14 km 163.5, 34149, Trieste, Italy

^eUniversità degli Studi di Parma, Parco Area delle Scienze 7/A, 43124, Parma, Italy.

*E-mail: roberta.ciprian@elettra.eu

Supplementary Information

Experimental Details

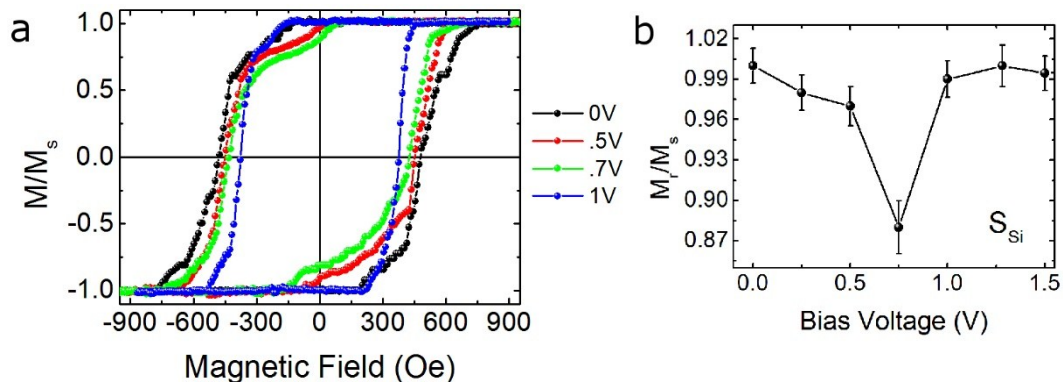
The system has been fabricated with a radiofrequency (RF) magnetron sputtering system, depositing simultaneously on polished polycrystalline Al₂O₃ (2 × 2 mm²) and thermally oxidised Si-(100) substrates (3 × 3 mm²). A Co layer, 100 nm thick, has been directly deposited on the substrates at room temperature (RT). Subsequently, a very thin and non-continuous Sn layer (a few angstroms thick) has been deposited. Sn acts as a catalyst for the growth of the ZnO NRs. The NRs have been fabricated at 400°C, via a self-assembly process, with a RF power of 150 W at 10⁻² mbar and a growing time of 300 s.¹⁻³ A schematic picture of the layer stack is reported in Fig. 1a of the main text. On top of Co, a layer of ZnO forms having a columnar/granular structure.² From this ZnO layer, the nanorods spontaneously develop, with the length and width determined by the sputtering deposition time. X-

ray diffraction data indicate that Co grew in its hcp structure, while ZnO shows a hexagonal wurtzite structure,¹ textured along the (001) direction.

The morphology of the multilayer has been investigated in cross section by a ZEISS Supra 40 field emission gun (FEG) scanning electron microscope (SEM) equipped with a Gemini column and an In-lens detector yielding an increased signal-to-noise ratio. Images were recorded collecting either secondary or backscattered electrons generated at 5 keV accelerating voltage.

Superconducting quantum interference device (SQUID) measurements have been carried out at 100 and 300 K in order to study the magnetic properties of the system with bulk sensitiveness.

Figure S11



(a) Hysteresis loops measured in longitudinal geometry on S_{Si} sample and (b) the corresponding M_r/M_s ratio as a function of the applied voltages in the range 0 – 1 V. The error bars have been evaluated from 15 hysteresis loops acquired at each voltage step.

X-ray Absorption Near Edge Spectroscopy (XANES) - Unpoled Sample

XANES spectra of the unpoled S_{A1} sample, acquired at the O K , Co and Zn $L_{2,3}$ edges are reported in Fig. SI2.

The spectra at the O K edge (Fig. SI2a) are characterised by two main features A_1 and A_2 in the 530-539 eV range, which stem from the hybridization of O $2p$ with dispersive Zn $4s$ and $4p$ states. The most intense A_2 peak is due to the transition of O $1s$ to more localised O $2p$ states.⁴⁻⁶ The A_1 pre-edge peak is sensitive to the formation and change in the amount of O vacancies (V_O) as well as to the Co/ZnO interdiffusion, which induces unoccupied $3d$ states inside the ZnO energy band gap.⁷ Features A_3 and A_4 in the 539-545 eV range can be ascribed to the hybridization of O $2p$ – Zn and Co $4p$ states, while those above 545 eV are assigned to O $2p$ – Zn $4d$ states.⁸ The absence of sharp peak in the low energy region (below 530 eV), typical of $3d$ oxides, is due to the fully-occupied Zn d^{10} configuration in ZnO, and the consequent absence of O $2p$ and Zn $3d$ hybridised states.⁹ In Co-doped ZnO compounds, this low-energy peak can also arise as a consequence of Co/ZnO intermixing which allows transitions from O $2s$ to hybridised O $2p$ – Co $3d$ states.^{7,10-}
¹¹ The absence of this feature, in particular in the spectra corresponding to α position (defined in Fig. 5a of the main text), suggests that the Co/ZnO interdiffusion is below the detection limit already at the Co/ZnO interface.

The O K spectrum acquired in α -point differs from that in β -point, characterised by the presence of ZnO nanorods. Indeed, the spectra for β have well defined and narrower spectral features, probably due to the contributions which arise from the nanorod tips and sidewalls,¹² contributions that are totally absent in point α . This is also in agreement with the increase in point β of the relative intensity of the most

intense peak A_2 with respect to A_1 , A_3 and A_4 features, an increase that is normally ascribed to ZnO nanostructures.^{8,13-14}

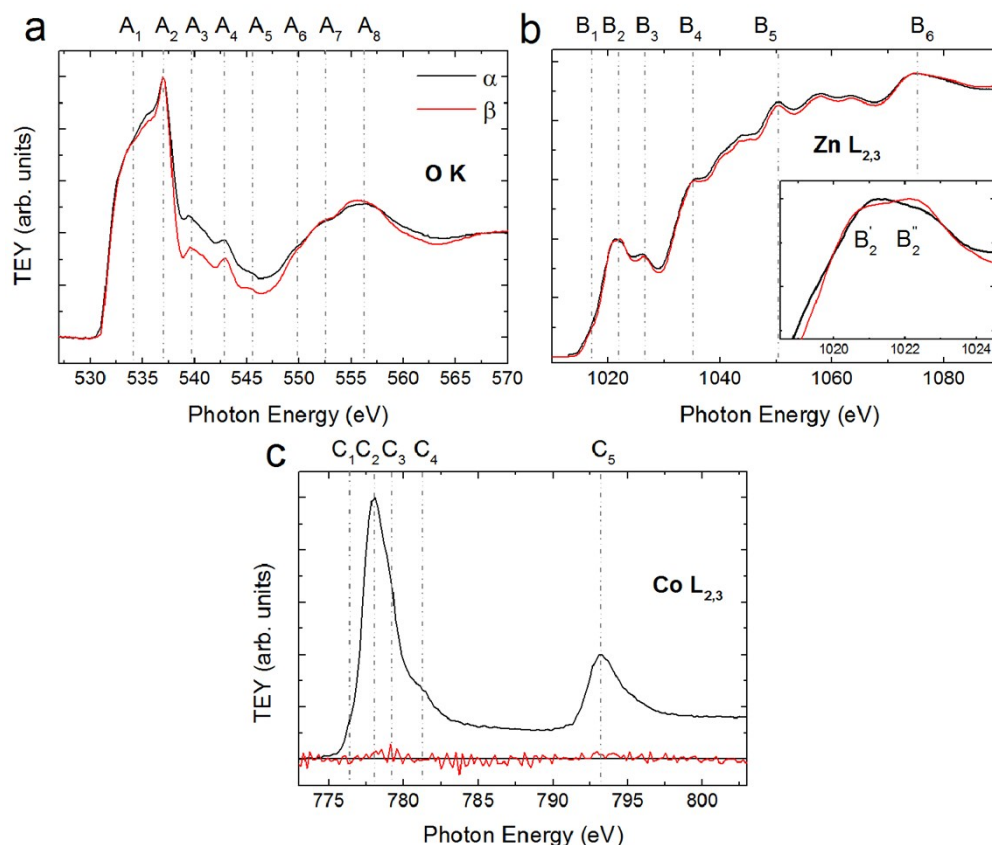


Figure SI2. XANES spectra acquired in point α and β indicated in Fig. 5a of the main text at (a) O K edge, (b) and (c) $L_{2,3}$ edges of Zn and Co, respectively.

Considering the difference in the image intensity scale in Fig. 5a of the main text, position β is clearly in the region where the ZnO are unaffected by the presence of Co, while the α -spectrum represents the Co/ZnO interface, affected by a huge strain due to the lattice mismatch.

Figure SI2b represents Zn $L_{2,3}$ -edge XANES spectra in the different sample positions. The Zn $3d$ orbital is fully occupied, and the lowest unoccupied state is Zn $4s$. Therefore, the spectral features between 1020 and 1035 (B_1 - B_3) are associated to transition from Zn $2p$ to $4s$ state as well as to antibonding $3d$ state.¹²⁻¹⁵ The spectrum

acquired for β differs from the α -spectrum. The inset shows the enlargement of the B_2 peak. This intense L_3 edge peak is constituted by two spectral features indicated as B_2' and B_2'' . The nanorods (position β) give rise to a shift of their positions towards slightly lower energy and to an inversion of the B_2' and B_2'' relative intensities.⁸

XANES spectra acquired at the Co $L_{2,3}$ edges (Fig. SI2c) are ascribed to metallic Co. The ZnO nanorods in point β prevented the detection of the Co signal. Indeed, as measurements were performed in total electron yield (TEY) mode, penetration depth was of few nm; thus, the Co/ZnO interface was too buried to be detected. On the contrary, in α point the absence of ZnO nanorods allows measuring the Co edges.

Figure SI3

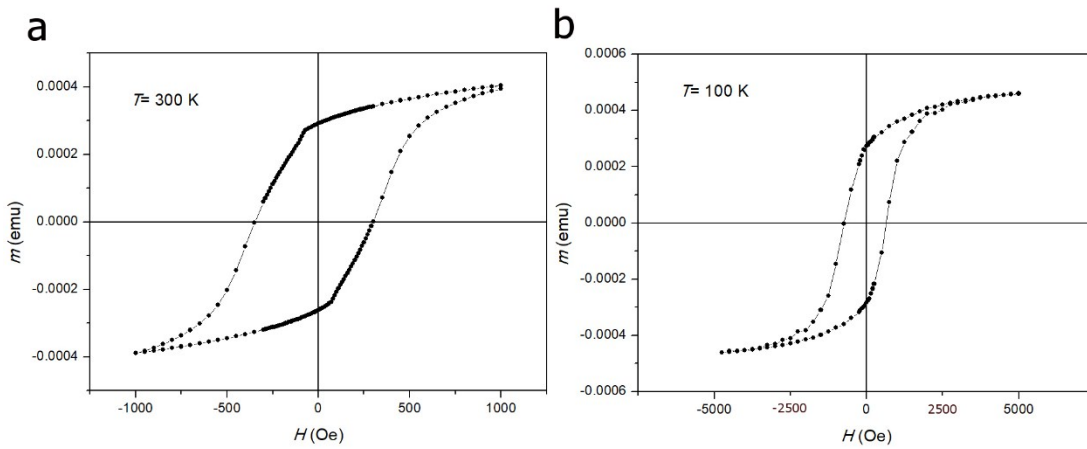


Figure SI3. SQUID hysteresis loops for S_{Al} acquired at (a) 300 and (b) 100 K.

References

- (1) R. Ciprian, C. Baratto, A. Giglia, K. Koshmak, G. Vinai, M. Donarelli, M. Ferroni, M., Campanini, E. Comini, A. Ponzoni, G. Sberveglieri, *RSC Adv.* 2016, **6**, 42517.
- (2) R. Ciprian, P. Torelli, A. Giglia, B. Gobaut, B. Ressel, G. Vinai, M. Stupar, A. Caretta, G. De Ninno, T. Pincelli, B. Casarin, G. Adhikary, G. Sberveglieri, C. Baratto, M. Malvestuto, *RSC Adv.* 2016, **6**, 83399.
- (3) P. Sundara Venkatesh, K. Jeganathan, *Cryst. Eng. Comm.* 2014, **16**, 7426.
- (4) S. Krishnamurthy, C. McGuinness, L. S. Dorneles, M. Venkatesan, J. M. D. Coey, J. G. Lunney, C. H., Patterson, K. E., Smith, T. Learmonth, P.-A. Glans, T. Schmitt, J.-H. Guo, *J. Appl. Phys.* 2006, **99**, 08M111.
- (5) J. G. Chen, *Surf. Sci. Rep.* 1997, **30**, 1.
- (6) C. Guglieri, E. Céspedes, A. Espinosa, M. Á. Laguna-Marco, N. Carmona, Y. Takeda, T. Okane, T. Nakamura, M. García-Hernández, M. Á. García, J. Chaboy, *Adv. Func. Mater.* 2014, **24**, 2094.
- (7) A. P. Singh, R. Kumar, P. Thakur, N. B. Brookes, K. H. Chae, W. K. Choi, *J. Phys.: Condens. Matter.* 2009, **21**, 185005.
- (8) P. Sundara Venkatesh, C. L. Dong, C. L. Chen, W. F. Pong, K. Asokan, K. Jeganathan, *Mater. Lett.* 2014, **116**, 206.
- (9) P. Thakur, K. H. Chae, J.-Y. Kim, M. Subramanian, R. Jayavel, K. Asokan, *Appl. Phys. Lett.* 2007, **91**, 162503.
- (10) S. Kumar, Y. J. Kim, B. H. Koo, H. Choi, C. G. Lee, S. K. Sharma, M. Knobel, S. Gautam, K. H. Chae, *J. Korean Phys. Soc.* 2009, **55**, 1060.
- (11) N. Srinatha, B. Angadi, K. G. M. Nair, N. G. Deshpande, Y. C. Shao, W.-F. Pong, *J. Electron. Spectrosc. Relat. Phenom.* 2014, **195**, 179.

- (12) J. W. Chiou, J. C. Jan, H. M. Tsai, C. W. Bao, W. F. Pong, M.-H. Tsai, I.-H. Hong, R. Klauser, J. F. Lee, J. J. Wu, S. C. Liu, *Appl. Phys. Lett.* 2004, **84**, 3462.
- (13) J. W. Chiou, K. P. Krishna Kumar, J. C. Jan, H. M. Tsai, C. W. Bao, W. F. Pong, F. Z. Chien, M.-H. Tsai, I.-H. Hong, R. Klauser, J. F. Lee, J. J. Wu, S. C. Liu, *Appl. Phys. Lett.* 2004, **85**, 3220.
- (14) S. B. Singh, Y.-F. Wang, Y.-C. Shao, H.-Y. Lai, S.-H. Hsieh, M. V. Limaye, C.-H. Chuang, H.-C. Hsueh, H. Wang, J.-W. Chiou, H.-M. Tsai, C.-W. Pao, C.-H. Chen, H.-J. Lin, J.-F. Lee, C.-T. Wu, J.-J. Wu, W.-F. Pong, T. Ohigashi, N. Kosugi, J. Wang, J. Zhou, T. Regier, T.-K. Sham, *Nanoscale* 2014, **6**, 9166.
- (15) M. Bibes, A. Barthélémy, *Nat. Mater.* 2008, **7**, 425.